

LETTER

Numerical Analysis of Monopole Multi-Sector Antenna with Dielectric Cylinder

Yuto SUZUKI^{†a)}, *Student Member* and Naoki HONMA[†], *Member*

SUMMARY This letter proposes a monopole multi-sector antenna with dielectric cylinder, and shows some results of simulations that examined the antenna characteristics. The dependency of radiation characteristics on relative permittivity ϵ_r shows the lens effect with increase of ϵ_r . Furthermore, the characteristics of the proposed antenna are improved by optimizing the termination conditions at the quiescent antennas. The backlobe level is lower than -10 dB. Also, the vertical HPBW and the conical HPBW are around 70.5° and 63.4° , respectively. The optimization improved the actual gain by 2 dB. It is found that the diameter of the proposed antenna is $1/3$ rd that of the conventional one.

key words: millimeter-wave band, lens antenna, multi-sector antenna, quiescent elements

1. Introduction

Recently, the data transmission rate is increasing in communication systems. The conventional communication system has limited access to the frequency bands. Millimeter wave (mm-wave) bands are many potentially available bands, such as $57 \sim 66$ GHz for transmission system [1]. Therefore, it is expected that mm-wave systems can realize very high transmission rates. Also, RF-systems can be easily miniaturized because the wavelength of mm-wave is short. Hence, System-On-Package (SOP) which is the integration of antenna and RF-system is proposed [2]. For such RF-systems, constructing the antenna within the dielectric substrate is useful because it can be easily configured with a high manufacturing accuracy.

However, high path loss at mm-wave is a serious problem since it degrades the communication quality. Therefore, a high-gain antenna is required to overcome this problem. A beam switchable antenna can be one of the solutions for achieving high gain to any direction and has been studied in many works [3]–[7]. But these antennas cannot be integrated with RF-system because their diameter is too large.

In this letter, a monopole multi-sector antenna with dielectric cylinder is proposed. The proposed antenna is constructed by several monopole elements, ground plane, and dielectric cylinder. The dependency of radiation characteristics on relative permittivity ϵ_r are analyzed to show the lens effect with increase of ϵ_r . Also, the effect of wavelength shortening in dielectric cylinder on the size of antenna is studied. Furthermore, the characteristics of the proposed an-

tenna are improved by optimizing the termination conditions at the quiescent antennas. It is clarified that the proposed antenna is effective in achieving switched-beam antenna that have compact configuration. In this study, Finite-Difference Time-Domain (FDTD) analysis is used to take account of the three dimensional dielectric components.

2. Proposed Antenna

Figure 1 shows a monopole multi-sector antenna with dielectric cylinder. The dielectric cylinder is arranged on the ground plane. Six monopole elements are uniformly arranged along the cylinder sidewall. Six-sector is assumed considering the simplification of the RF-circuit. The monopoles can be configured by using through holes in the substrate. Dielectric has the two effects. One is able to focus radio wave such as lens, and the other is that shortening wavelength. These effects achieve high-gain and miniaturized antenna. The directivity can be controlled by switching the feed port.

The antenna elements except the feed antenna are unconnected to the feed line. Therefore, these elements can be regarded as the quiescent antennas. In this study, the quiescent antennas are used to improve the radiation characteristics. The reactive loads are connected to the quiescent antenna ports. The current on the quiescent antennas is changed by the reactive loads. Hence, the directivity of the proposed antenna is changed. Also, the reactive loads at the quiescent antenna ports are switched when the feed port is switched. Therefore, the similar directivity can be obtained when each antenna element is fed.

ESPAR antenna, whose feed element is at the center

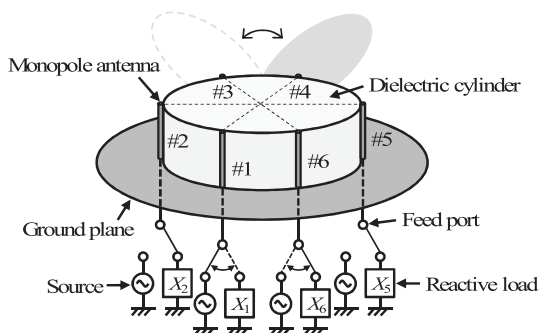


Fig. 1 Structure of monopole multi-sector antenna with dielectric cylinder.

Manuscript received January 27, 2012.

Manuscript revised May 8, 2012.

[†]The authors are with the Graduate School of Engineering, Iwate University, Morioka-shi, 020-8551 Japan.

a) E-mail: t2311036@iwate-u.ac.jp

DOI: 10.1587/transcom.E95.B.2991

of the circular parasitic antennas, has similar configuration, but its maximum actual gain is lowered to 4.26 dBi when it is configured in the dielectric material [8]. The feed element in the proposed antenna is arranged along the cylinder sidewall. The dielectric cylinder and other quiescent elements work together like the director in Yagi-Uda antenna. By this effect, the high actual gain can be achieved even when the antenna is configured within the substrate.

3. Optimization Method

In the following optimization method, the iterative verification of the directivity is required, but it will cost significant CPU time for the total process. In this study, the directivity is calculated by the directivity synthesis method [9]. Thus, the directivities with certain loads are estimated by post processing with very small computation time.

The feed antenna is connected to a 50Ω feed line. The quiescent antennas are connected to the reactive loads, $\mathbf{X} = (X_2, X_3, \dots, X_6)$. The quiescent antennas at the symmetrical positions are connected to same reactive loads, i.e., $X_2 = X_6$ and $X_3 = X_5$. The reason includes the realization of symmetrical beam on the azimuth plane, and easy fabrication of the RF-circuit by reducing the number of the reactive loads. The reactive loads are optimized evaluating the radiation characteristics of the proposed antenna. The radiation characteristics are evaluated using the steepest gradient method [10]. Now define F_1^k as the evaluation function of the 1st antenna port at k step. The gradient can be expressed as

$$\mathbf{g}_1^k = \left(\frac{\partial F_1^k}{\partial X_2}, \frac{\partial F_1^k}{\partial X_3}, \dots, \frac{\partial F_1^k}{\partial X_6} \right), \quad (1)$$

where ∂X_i is the minor change of the reactance. Next, define \mathbf{X}^k and \mathbf{X}^{k+1} as the reactances at k and $k+1$ steps, respectively. The reactances for step $k+1$ can be expressed as $\mathbf{X}^{k+1} = \mathbf{X}^k + \alpha \mathbf{g}_1^k$, where α is the constant to climb the gradient. Thus, the gradient is considered to next step reactances. Therefore, reactances will approach to an optimal value step by step.

By using the steepest gradient method, it tends to be optimized to the specific parameter by the setting of the evaluation function. For example, the antenna can be mainly optimized for a certain property, such as gain, sidelobes, and so on, and it ends up with the antenna having unwanted characteristics. One of the solutions for this is setting the physically feasible goal for the optimization process. To design the sector antenna, the beam shape of the mainlobe is important. In this study, the reference HPBWs (Half-Power Beam Widths) are defined in advance. The reference gain is calculated by

$$G_0 = \frac{K}{\theta_0 \phi_0}, \quad (2)$$

where K is the constant which determine by the aperture shape and the distribution of electromagnetic on the aperture plane, θ_0 is the reference HPBW on the vertical plane, and

ϕ_0 is the reference HPBW on the conical plane [11]. The conical plane is defined in the plane with the mainlobe and that θ is the constant [7]. In this simulation, the parameters are set to $K = 3.4 \times 10^4$, $\theta_0 = 70^\circ$, and $\phi_0 = 60^\circ$ considering circular aperture and six-sector.

The evaluation function is calculated by the gain, the conical HPBW, and the F/B (front-to-back ratio). The gain of the antenna is the most important factor in the evaluation function since the path loss in the mm-wave bands is very high. The term for gain is expressed as

$$f_g = -|G_t - G_0|, \quad (3)$$

where G_t is the gain when \mathbf{X} is given to the quiescent antenna ports. Next, in order to consider the sector beam-shape, the conical HPBW is the necessary factor in the evaluation function. The term for HPBW is expressed as

$$f_\phi = -|\phi_t - \phi_0|, \quad (4)$$

where ϕ_t is the HPBW on the conical plane when changed the reactive loads. Thus, f_g and f_ϕ become maximum if G_t and ϕ_t approach to G_0 and ϕ_0 , respectively. Here, ϕ_0 is 60° since this is the six sector antenna. The F/B is also taken into account in the evaluation function because the suppression of the undesired radiation can yields high-gain. The term for F/B is expressed as f_{FB} , which is set to $-F/B$. The evaluation function is expressed as

$$F = w_g f_g + w_\phi f_\phi + w_{FB} f_{FB}, \quad (5)$$

where w_g , w_ϕ , and w_{FB} are the weights to converge to the desired characteristics, and are set to be independent of the steps and the initial reactances. The absolute values of the terms for gain and F/B are multiplied by w_g and w_{FB} , respectively. w_ϕ is needed to be larger value than other values because the conical HPBW has small change against the change of reactance.

4. Numerical Analysis

Figure 2 shows the analysis model. Six monopole elements are uniformly arranged along the cylinder sidewall. #1 is the feed antenna, and the others are the quiescent antennas. It is assumed that all elements are connected to a 50Ω feed

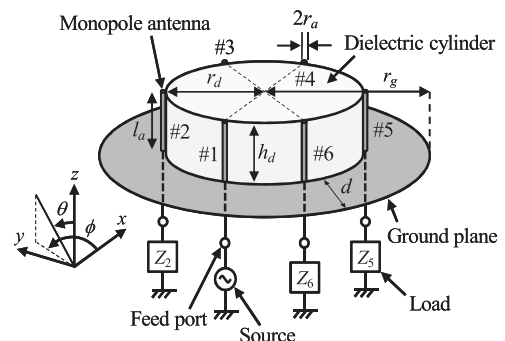
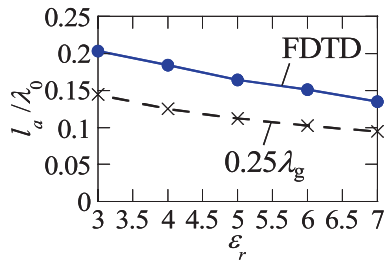


Fig. 2 Analysis model.

Table 1 Analysis conditions.

Center frequency	60 GHz
Analysis frequency	57 ~ 63 GHz
Number fo time step	32768
Feed model	Delta-gap feed
Exciting pulse	Gaussian pulse
Absorbing B.C.	PML 8-layers

**Fig. 3** Antenna length versus ϵ_r .

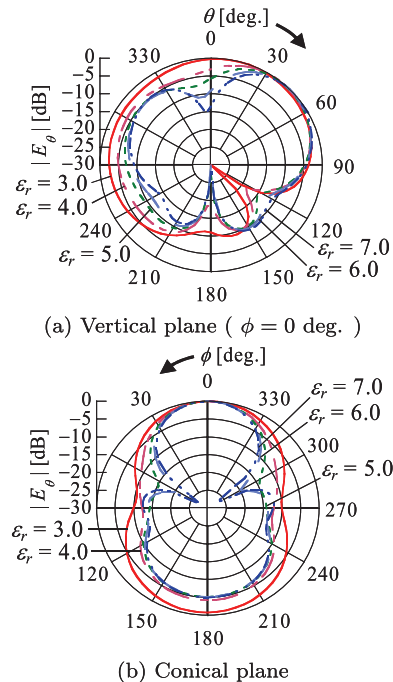
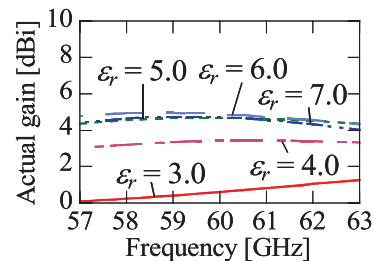
line before the optimization, i.e., $Z_i = 50 \Omega$. h_d and r_d are the height and the radius of the dielectric cylinder, respectively. l_a and r_a are the length and the radius of the antenna element, respectively. d is the distance between the edge of the ground plane and the dielectric cylinder. r_g is the radius of the ground plane. For simplification, we assumed $h_d = l_a$ and neglected the thickness of the ground plane. The dimensions are set to $r_d = 0.25\lambda_0$, $r_a = 0.02\lambda_0$, $d = 0.25\lambda_0$, and $r_g = r_d + d$, where λ_0 is the wavelength in vacuum. Details of the FDTD analysis configurations are summarized in Table 1. The shape of the cell is the cubic.

Figure 3 shows the antenna lengths for the relative permittivity ϵ_r of the dielectric cylinder. ϵ_r is set to $3.0 \leq \epsilon_r \leq 7.0$. λ_g is the effective wavelength, calculated as $\lambda_g = \lambda_0 / \sqrt{\epsilon_r}$. Dot-line is the antenna length obtained by FDTD analysis considering the matching. The antenna length obtained by FDTD analysis is longer than $0.25\lambda_g$. It means that the finite dielectric, the finite ground plane, and the quiescent antennas have an impact on the effective wavelength. In the following numerical analysis, the antenna length obtained by FDTD analysis is used.

Figure 4 show the radiation patterns at 60 GHz for various relative permittivities. Where, the electric field, $|E_\theta|$, is the normalized by the maximum value. From the result in Fig. 4(a), it can be confirmed that the mainlobe is tilted in the horizontal direction. Also, from the result in Fig. 4(b), the narrow beam can be formed. Furthermore, the F/B increases when ϵ_r becomes large, but doesn't become higher than 10 dB.

Figure 5 shows the actual gain versus the frequency for various relative permittivities. It can be confirmed that the actual gain is increased by increase of ϵ_r . However, the actual gain is not changed by increasing more than $\epsilon_r = 5.0$. The result in Fig. 3 means that the lens effect of the dielectric cannot be effective in the gain because the antenna structure becomes smaller.

Based on the results shown above, the dielectrics with $\epsilon_r = 5.0$ is used in the following discussion. The termi-

**Fig. 4** Radiation patterns at 60 GHz for various ϵ_r .**Fig. 5** Actual gain versus frequency for various ϵ_r .

nations of the quiescent antenna ports must be optimized to obtain more desirable characteristics. The reactive loads are connected to the quiescent antenna ports, i.e., $Z_i = jX_i$. 1000 trials with different initial reactance sets are examined to avoid the local maximum. These sets are generated randomly with the range, $-50 \leq X_i \leq 50 \Omega$. For example, the reactive loads can be constructed by the stubs on the dielectric substrate. The actual reactance contains the error because of the manufacturing error. The reactance error becomes higher when the absolute value of reactance becomes larger. The reactances between -50 and $+50 \Omega$ have a relatively small effect on the reactance error. Therefore, the ranges of the reactive loads are selected from -50 to $+50 \Omega$. α is set to 100. Number of iterative computation is 100. The weights are set to $w_g = 100$, $w_\phi = 1000$, and $w_{FB} = 10$.

Figure 6 show the radiation patterns at 60 GHz. It can be seen that the backlobe level is lower than -10 dB by optimizing the reactive loads at the quiescent antenna ports. Also, the vertical and conical HPBWs are much wider to 70.5° and 63.4° , respectively. Furthermore, The F/B becomes higher than 11 dB.

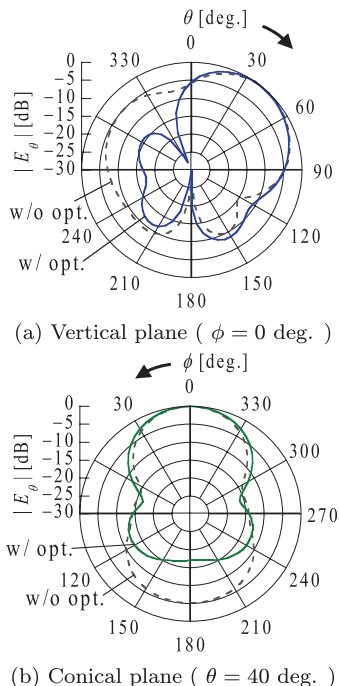


Fig. 6 Radiation patterns at 60 GHz.

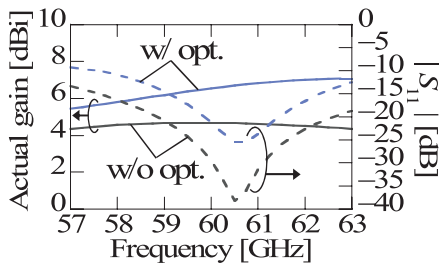


Fig. 7 Actual gain and $|S_{11}|$ versus frequency.

Figure 7 shows the actual gain and $|S_{11}|$ versus frequency. It can be seen that the feed port is matched enough to $50\ \Omega$ feed line even when the quiescent antenna ports are terminated by the reactive loads. It is found that the actual gain of the optimized antenna is 6.54 dBi at 60 GHz that is 2 dB higher than the gain without the optimization, and it outperforms the gain of the work [8].

The proposed antenna size is compared to the conventional one [7]. It is found that the diameter of the proposed antenna is 1/3rd that of the conventional one. Therefore, the proposed antenna is effective in downsizing the switched-beam antenna.

5. Conclusion

In this letter, a monopole multi-sector antenna with dielec-

tric cylinder has been proposed. The radiation characteristics for relative permittivity ϵ_r of the dielectric cylinder were analyzed. It showed the lens effect with increase of ϵ_r . Furthermore, by optimizing the termination conditions at the quiescent antennas, the backlobe level is lower than -10 dB at 60 GHz. Also, the vertical and conical HPBWs are around 70.5° and 63.4°, respectively. The optimization improved the actual gain by 2 dB. It is found that the diameter of the proposed antenna is 1/3rd that of the conventional one. These results proved that the proposed antenna is effective in achieving switched-beam antenna that have compact configuration.

References

- [1] S.K. Yong and C.-C. Chong, "An overview of multigigabit wireless through millimeter wave technology: Potentials and technical challenges," *EURASIP J. Wireless Communications and Networking*, vol.2007.
- [2] K. Lim, S. Pintel, M. Davis, A. Sutono, C.-H. Lee, D. Heo, A. Obatoynbo, J. Laskar, E.M. Tantzeris, and R. Tummala, "RF-system-on-package (SOP) for wireless communications," *IEEE Microw. Mag.*, vol.3, no.1, pp.88-99, March 2002.
- [3] T. Maruyama, K. Uehara, T. Hori, and K. Kagoshima, "Rigorous analysis of transient radiation mechanism of small multi-sector monopole Yagi-Uda array antenna using FDTD method," *Int. J. Numerical Modeling*, vol.12, no.4, pp.341-351, 1999.
- [4] T. Seki and T. Hori, "Cylindrical multi-sector antenna with self-selecting switching circuit," *IEICE Trans. Commun.*, vol.E84-B, no.9, pp.2407-2412, Sept. 2001.
- [5] M. Yamamoto, K. Ishizaki, M. Muramoto, K. Sasaki, and K. Itoh, "A planar-type five-sector antenna with printed slot array for millimeter-wave and microwave wireless LANs," *IEICE 2000 Int. Symp. Antenna and Propagation*, vol.1, pp.206-208, Aug. 2000.
- [6] N. Tenno, A. Miura, T. Itoh, M. Taromaru, and T. Ohira, "A fundamental study on a switched-beam sector slot-array antenna in 60GHz band," *Int. Symp. on Antennas and Propagat.*, Singapore, Nov. 2006.
- [7] N. Honma, T. Seki, K. Nishikawa, K. Tsunekawa, and K. Sawaya, "Compact six-sector antenna employing three intersecting dual-beam microstrip Yagi-Uda arrays with common director," *IEEE Trans. Antennas Propag.*, vol.54, no.11, pp.3055-3062, Nov. 2006.
- [8] Q. Han, B. Hanna, and T. Ohira, "A compact espar antenna with planar parasitic elements on a dielectric cylinder," *IEICE Trans. Commun.*, vol.E88-B, no.6, pp.2284-2290, June 2005.
- [9] Y. Suzuki, M. Obara, and N. Honma, "Radiation pattern optimization using quiescent elements in circular array antenna with cylindrical dielectric load," *Int. Symp. on Antennas and Propagat.*, Jeju, Oct. 2011.
- [10] J.W. Bandler, "Optimization methods for computer-aided design," *IEEE Trans. Microw. Theory Tech.*, vol.MTT-17, no.8, pp.533-552, Aug. 1969.
- [11] J.D. Kraus, *Antennas*, 2nd ed. McGraw-Hill Electrical Engineering Series, New York, 1988.